Hindawi
International Journal of Antennas and Propagation
Volume 2017, Article ID 1957572, 13 pages
https://doi.org/10.1155/2017/1957572

Research Article

Assessment Method of Multipath Mitigation Performance for GNSS Antenna with Receiver Algorithms

Muzi Yuan, Du Li, Baiyu Li, Huaming Chen, and Gang Ou

College of Electronic Science and Engineering, National University of Defense Technology, 109 Deya Road, Changsha, China

Correspondence should be addressed to Muzi Yuan; muzi.yuan@outlook.com

Received 9 March 2017; Revised 26 April 2017; Accepted 3 May 2017; Published 18 September 2017

Academic Editor: Stefania Bonafoni

Multipath is one of the most important sources of positioning error in GNSS. Well-designed antennas can mitigate multipath signals and enhance the performance of GNSS receivers. This paper concentrates on methods to assess multipath mitigation performance for GNSS antennas. We propose a model to describe multipath environment in GNSS ground stations. The model analyzes effects caused by inclined reflective surfaces and multipath mitigating algorithms in receivers. A method to assess multipath mitigation performance is put forward by analyzing pseudorange code phase errors caused by multipath signals after signal processing. Based on the model and method, principles in site selection for GNSS antenna are introduced to minimize effects caused by multipath.

1. Introduction

Global Navigation Satellite System (GNSS) plays a significant role in military, industry, and civil field. In GNSS the precision of pseudorange measurement is highlighted in most applications. Pseudorange error has impact on both availability and integrity of navigation and positioning. Among all the factors that may cause pseudorange error, multipath is one of the factors that cannot be compensated for by observations provided by monitoring data [1]. Multipath signals are additional signal replicas generated by reflection in local environment. These duplicated signals may introduce a bias in delay lock loops (DLLs) of GNSS receivers, which finally leads to an increase in pseudorange error [2]. To mitigate the impact of multipath, theories and algorithms are proposed. There are mainly two approaches in multipath mitigation. One approach is to manipulate radiation patterns of antennas. The other is to redesign how receivers handle the incoming signal.

Because the model of multipath signal is an important reference to multipath mitigation, it should be studied first. Pattern of multipath signals in different multipath environments was studied in [3]. However, only horizontal reflective surfaces are considered in the research. Physical studies were performed on GPS multipath caused by land reflection in [4, 5]. Pattern of multipath signals reflected from horizontal soil land was analyzed and effects of soil moisture were discussed. A method to estimate multipath signal was put forward with electromagnetic modeling [6]. The technology offered a detailed model of multipath signals. Model of multipath signals in GNSS monitoring stations can be studied by methods mentioned above.

To mitigate multipath signals in signal processing stage, many algorithms were proposed. The narrow correlator spacing method [7] is one of the approaches to mitigate multipath by reducing the chip spacing between the early and late correlators. However, the sensitivity to noise of this method is high and multipath signals with short delay cannot be mitigated well. A method was put forward to reduce the impact of multipath by employing a four-correlator structure called the early-late slope [8]. Then the algorithm was simplified by researchers in Ashtech [9], Ohio University [10], NovAtel [11], and Leica [12] and called double-delta [13]. The multipath estimating delay lock loop (MEDLL) [14] algorithm was proposed based on the maximum likelihood (ML) estimation. The algorithm estimates the delay and the power of all possible paths by studying the shape of the cross-correlation function. However, short delay multipath

mitigation is still an issue. Based on maximal measurement tree (MMT) algorithm, vision technology [15] was proposed to evaluate the parameters of both direct signal and multipath signal by iteration. A Bayesian approach [16] was proposed for GNSS receivers to mitigate multipath by prior information of the satellite signal. However, in practice it is usually difficult to access prior information. More recently the maximum likelihood estimator based on a Newton type technique was implanted to mitigate multipath delay [17].

Algorithms mentioned above focus on signal processing in receivers and provide general conclusions of multipath mitigation performance. Every method has disadvantages in multipath mitigation or accessibility. Meanwhile multipath mitigation provided by antenna is ignored. Effect of multipath mitigation antenna can be a reinforcement for multipath mitigation.

The most widespread method to evaluate the performance of multipath mitigation for antennas is the front-to-rear ratio [18]. The ratio is the power gain of the same angle in front and rear side. It is an ambiguous indicator because only multipath signals caused by horizontal surfaces have the same angle as direct signal.

Hence it is necessary to develop an accurate assessment method for antennas. This paper concentrates on antennas sited at ground stations. A model of multipath environment in ground station is provided and assessment method for antennas is developed. Data measured from real antennas is adopted to demonstrate the assessment method and the dependence of site selection.

The rest of this paper is organized as follows. In Section 2, model of multipath environment is discussed. A progressed model involving inclined reflective surface is studied. In Section 3, multipath mitigation algorithms in receivers are analyzed and the effect to the performance of the whole system is discussed. In Section 4, an assessment method is put forward to approach a precise evaluation for multipath mitigation. In Section 5, the dependence of the site of antenna is discussed using data of actual antennas. Principles are provided to achieve better multipath mitigation performances. In Section 6, we discuss the availability of the proposed method under other algorithms or modulations.

2. Multipath Model in Semiopen Land

In this section, an antenna located at the center of a semiopen land is discussed. Semiopen land refers to an area with no inclined mirror reflective surface within a radius range of S_0 in horizontal distance from the antenna. There are inclined reflective surfaces with random dip angles out of the range S_0. This environment description can simulate the multipath environment near monitoring stations. This kind of environment can be demonstrated as in Figure 1.

Propagation delay of the multipath signal is related to the difference in path length between direct signal and its multipath replica. Difference in path length can be calculated via geometry in Figure 1. We use $\Delta\tau$ to denote the propagation

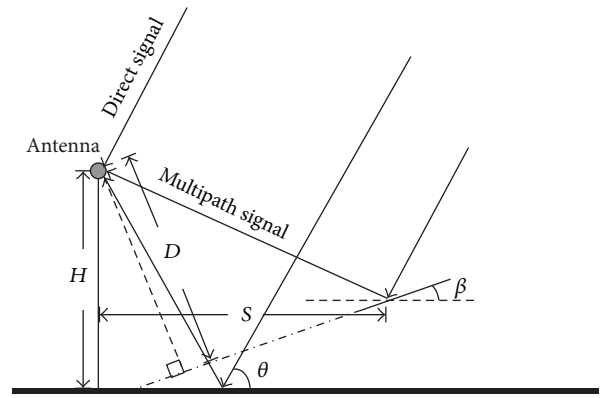

Figure 1: This figure shows how multipath signal is produced. Multipath signals are mainly produced by two kinds of reflective surfaces: horizontal surfaces and inclined surfaces. Elevation angles of multipath signals caused by horizontal surfaces equal to negative elevation angles of direct signals. Elevation angles of multipath signals caused by inclined surfaces depend on both the elevation angles of direct signals and the dip angles of the surfaces.

delay of multipath signal. Equation (1) shows how the property of reflection surface affects $\Delta\tau$.

$$\Delta\tau = \frac{2D \cdot \sin(\theta - \beta)}{c}. \tag{1}$$

Here D is the vertical distance between antenna and reflective surface, θ is the elevation angle of the direct signal, β is the dip angle of the surface, and c is the speed of light. In practice elevation angles of direct signals are the same as elevation angles of satellites.

2.1. Horizontal Surfaces. When dip angle β of a surface satisfies $\beta = 0$, we call the surface a horizontal surface. Propagation time delay at this kind of surfaces can be simplified as

$$\Delta\tau = \frac{2H \cdot \sin(-\varphi_m)}{c}. \tag{2}$$

In this case φ_m is the elevation angle of multipath signal. In practice antennas are installed above the ground. So $\varphi_m < 0$ is satisfied.

While the width of the pseudo-random noise code (PRN code) correlation peak is the same as the chip width T_c of the PRN code, any multipath signals with delays more than T_c have no impact on the correlator. Hence the propagation time delay is restricted within $0 < \Delta\tau < T_c$. So, the restriction of multipath signal elevation angle φ_m satisfies

$$-\arcsin\left(\frac{c \cdot T_c}{2H}\right) < \varphi_m < 0. \tag{3}$$

2.2. Inclined Surfaces. Since dip angles β of some surfaces are $\beta \neq 0$, we call these surfaces inclined surfaces. Propagation

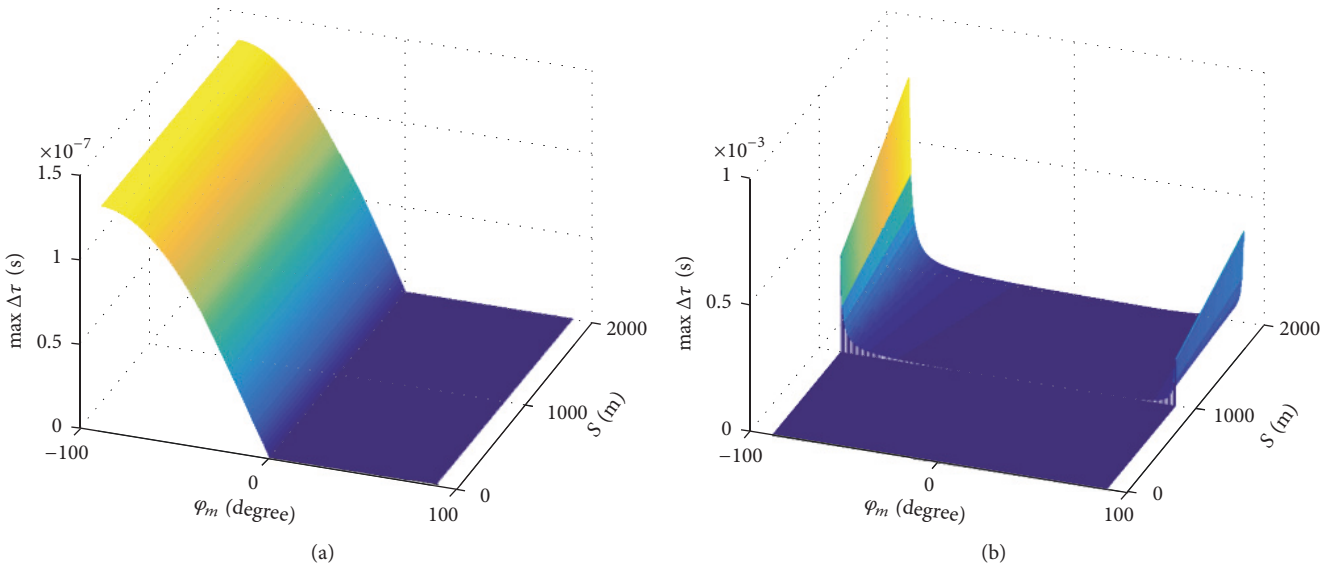

FIGURE 2: In this figure, the height H of the antenna is set to 20 m and the radius S_0 of the semiopen land is 2000 m. (a) shows propagation time delays of multipath signals produced by horizontal surfaces. The delay is only relative to the elevation angle of the direct signal. (b) shows propagation time delays of multipath signals produced by inclined surfaces. The delay increases by the distance S and the absolute value of elevation angle φ_m.

time delay is relative to the dip angle of the surface, the distance from the surface to the antenna, and the elevation angle of the direct signal. Equation (4) shows the vertical distance D from the surface to the antenna.

$$D = S \cdot \frac{\sin(\theta - \beta)}{\cos(\theta - 2\beta)}. \tag{4}$$

This vertical distance can be transformed into geometry distance for propagation time delay calculation. Hence the multipath propagation time delay $\Delta\tau$ caused by inclined reflective surfaces can be represented by

$$\Delta\tau = \frac{2S}{c} \cdot \frac{\sin^2(\theta - \beta)}{\cos(\theta - 2\beta)}. \tag{5}$$

The elevation angle of the multipath signal is $\varphi_m = 2\beta - \theta$. It indicates that when the elevation angle of the satellite increases from 0 to $\pi/2$, the elevation angle of multipath signals varies from 2β to $2\beta - \pi/2$. When $\theta < \beta$, the propagation time delay of multipath signals decreases with the increase of satellite elevation angles. The relation between φ_m, θ, and $\Delta\tau$ can be shown as

$$\Delta\tau = \frac{2S}{c} \cdot \frac{\sin^2((\theta - \varphi_m)/2)}{\cos(\varphi_m)}. \tag{6}$$

When elevation angles of multipath signals are negative, time delays increase by satellite elevation angles.

Let H_m be the height of the inclined surface, which is restricted by

$$H_m = H + S \cdot \tan(\varphi_m). \tag{7}$$

Here H is the installation height of the antenna. In the situation when signals reflect at surfaces lower than antennas, H_m and S are restricted by $0 < H_m < H$ and $S > S_0$. Elevation angles of multipath signals are restricted by

$$-\arctan\left(\frac{H}{S_0}\right) < \varphi_m < 0. \tag{8}$$

Surfaces higher than antenna will produce multipath signals with positive elevation angles.

2.3. Model Characteristics. Propagation time delays of multipath signals can be demonstrated in Figure 2. In the environment described above, horizontal surfaces produce multipath signals with low propagation time delays while high propagation time delays are produced by inclined surfaces.

Under the environment of GNSS monitoring station, elevation angles of multipath signals are restricted. There are only multipath signals with elevation angles larger than

$$\min\left[-\arcsin\left(\frac{c \cdot T_c}{2H}\right), -\arctan\left(\frac{H}{S_0}\right)\right]. \tag{9}$$

A connection between elevation angles of multipath signals and the multipath model of environment is established by geometry tools and the assumption of semiopen land.

3. Effects of Multipath Mitigation Algorithms

In this section, effects of multipath mitigation algorithms deployed in receivers are analyzed. Double-delta algorithm is picked up as an example. Principles of the algorithm will not be discussed in this paper. Detailed process of derivation has been shown in [8–13]. Formulas and conclusions of algorithms are provided directly for convenience in this section.

The direct signal can be represented by

$$r_d = A_{\text{direct}} \cdot p\left(t - \tau_0\right) \cdot \cos\left(2\pi f t + \phi_0\right). \tag{10}$$

A typical multipath signal can be represented by

$$\begin{aligned} r_m = {} & \alpha \cdot A_{\text{direct}} \cdot p\left(t - \tau_0 - \Delta\tau\right) \\ & \cdot \cos\left(2\pi f t + \phi_0 + \Delta\phi\right). \end{aligned} \tag{11}$$

Here $\alpha = A_{\text{multipath}}/A_{\text{direct}}$ is the amplitude ratio of the direct signal and the multipath signal. τ_0 is the propagation time delay from the satellite to the receiver. $\Delta\tau$ is the time delay of the multipath signal, $p(t)$ is the baseband signal, f is the frequency of carrier, ϕ_0 is the initial phase of the carrier, and $\Delta\phi$ is the phase shift in the carrier of the multipath signal. Mean difference between multipath signals and direct signals is their different amplitudes, PRN code phases, and carrier phases.

In this case, signals in receivers can be represented as a combination of direct signals and multipath signals. r_d is used to denote the direct signal, r_m denotes the multipath signal, and r is used to denote the received signal.

$$r = r_m + r_d. \tag{12}$$

The double-delta algorithm employs two pairs of correlators E2, E1 in leading phase and L1, L2 in lag phase. There is a $d/2$ delay in E2-E1 and L1-L2. Here d is also the early-late space between correlators E1 and L1. Those two pairs of correlators are assigned by the same early-late spacing $d/2$ and ordered as E2, E1, L1, and L2. There is a $2d$ spacing between correlator E2 and correlator L2. Slopes of both sides of the correlation peak can be measured by these two pairs of correlators. A brief demonstration of correlators is shown in Figure 3(a). In this case the PRN code phase evaluation function of double-delta algorithm is shown in

$$\widehat{\varepsilon} = D\left(\varepsilon\right) = \text{IR}_{\text{E1}}\left(\varepsilon\right) - \text{IR}_{\text{L1}}\left(\varepsilon\right) - \frac{\text{IR}_{\text{E2}}\left(\varepsilon\right) - \text{IR}_{\text{L2}}\left(\varepsilon\right)}{2}. \tag{13}$$

Here $\widehat{\varepsilon}$ is the PRN code phase evaluation; $\text{IR}_x(\varepsilon)$ is the output of correlator x at phase shift ε. Mark x stands for E2, E1, L1, or L2. Combining multipath signal model and phase evaluation function, the PRN code phase error (PPE) can be represented by the following [20]:

$$\begin{aligned} & \varepsilon\left(\alpha, \Delta\tau, \Delta\phi\right) \\ & = \begin{cases} \dfrac{\alpha\Delta\tau \cdot \cos\left(\phi_e + \Delta\phi_0\right)}{1 + \alpha\cos\left(\phi_e + \Delta\phi_0\right)} & 0 < \Delta\tau \le \tau_A \\ \dfrac{\alpha\left(d - \Delta\tau\right) \cdot \cos\left(\phi_e + \Delta\phi_0\right)}{1 - \alpha\cos\left(\phi_e + \Delta\phi_0\right)} & \tau_A < \Delta\tau \le d \\ 0 & d < \Delta\tau \le T_c - d \\ \dfrac{\alpha\left(d - T_c + \Delta\tau\right) \cdot \cos\left(\phi_e + \Delta\phi_0\right)}{2 + \alpha\cos\left(\phi_e + \Delta\phi_0\right)} & T_c - d < \Delta\tau \le \tau_B \\ \dfrac{\alpha\left(T_c - \Delta\tau\right) \cdot \cos\left(\phi_e + \Delta\phi_0\right)}{2 - \alpha\cos\left(\phi_e + \Delta\phi_0\right)} & \tau_B < \Delta\tau \le \tau_C \\ \dfrac{\alpha\left(-d - T_c + \Delta\tau\right) \cdot \cos\left(\phi_e + \Delta\phi_0\right)}{2 + \alpha\cos\left(\phi_e + \Delta\phi_0\right)} & \tau_C < \Delta\tau \le T_c + d \\ 0 & \Delta\tau > T_c + d. \end{cases} \end{aligned} \tag{14}$$

Here τ_A, τ_B, and τ_C are defined by

$$\begin{aligned} \tau_A &= \frac{d}{2} \cdot \left[1 + \alpha\cos\left(\phi_e + \Delta\phi_0\right)\right], \\ \tau_B &= \frac{\alpha d}{4} \cdot \cos\left(\phi_e + \Delta\phi_0\right) + T_c - \frac{d}{2}, \\ \tau_C &= -\frac{\alpha d}{4} \cdot \cos\left(\phi_e + \Delta\phi_0\right) + T_c + \frac{d}{2}. \end{aligned} \tag{15}$$

Here $\Delta\phi = \phi_e + \Delta\phi_0$ is the carrier phase difference between direct signals and multipath signals, ϕ_e is the phase shift in the process of reflection, and $\Delta\phi_0$ is the phase difference provoked by the different path length between direct signals and multipath signals. d is the early-late spacing between correlator E1 and L1; T_c is the chip width of the PRN code. The structure of the correlators in double-delta and the performance in multipath mitigation of the algorithm are shown in Figure 3.

It can be found in Figure 3(b) that performance of the algorithm upgrades when the early-late spacing decreases. However, a small early-late spacing may degrade the performance of the algorithm when noise is considered in it. Hence, in this paper, d is set to $0.25T_c$ to maintain noise resistance while acquiring an enough performance for multipath mitigation.

Double-delta algorithm can effectively mitigate PPE caused by multipath signal when multipath delay meets the condition that $d < \Delta\tau \le T_c - d$. Elevation angles of those multipath signals can be calculated by conclusions in Section 2. Multipath signals with delay over $T_c + d$ have no impact on PPE. Hence multipath signals with some specific elevations can be ignored.

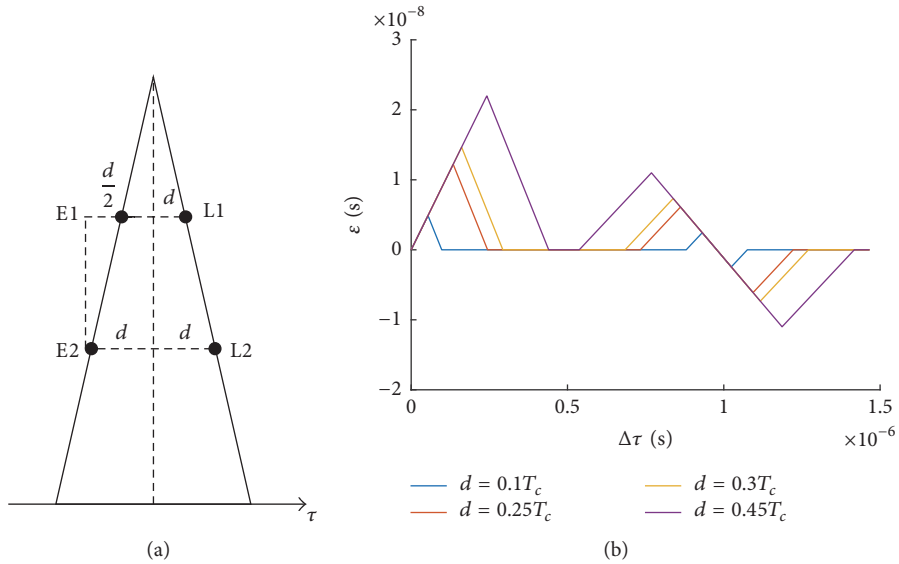

FIGURE 3: This figure shows the structure and the performance of the double-delta algorithm. (a) is the assignment of two pairs of correlators in double-delta algorithm. (b) is a plot of (14) where $\Delta\phi = \phi_e + \Delta\phi_0$ is set to 0 for simplification. In the plot, T_c is set to $1/1.023e6$ as the chip width of GPS C/A code; $\alpha = A_{\text{multipath}}/A_{\text{direct}}$ is set to 0.3 for demonstration. The plot shows PPE under different d in double-delta algorithm.

At horizontal surfaces ($\beta = 0$), elevation angles of multipath signals with delays within the conditions above can be represented as

$$\begin{aligned} -\arcsin\left(\frac{cd}{2H}\right) &< \varphi_m < 0, \\ -\arcsin\left(\frac{c\left(T_c+d\right)}{2H}\right) &< \varphi_m \\ &< -\arcsin\left(\frac{c\left(T_c-d\right)}{2H}\right). \end{aligned} \tag{16}$$

At inclined surfaces ($\beta \neq 0$) condition restriction formula is used to describe the elevation by

$$\begin{aligned} 0 &< \frac{\sin^2\left(\left(\theta-\varphi_m\right)/2\right)}{\cos\left(\varphi_m\right)} < \frac{cd}{2S_0}, \\ \frac{c\left(T_c-d\right)}{2S_0} &< \frac{\sin^2\left(\left(\theta-\varphi_m\right)/2\right)}{\cos\left(\varphi_m\right)} < \frac{c\left(T_c+d\right)}{2S_0}. \end{aligned} \tag{17}$$

According to Section 2, φ_m meets the restriction in

$$\begin{aligned} \varphi_m \in &\left(\min\left\{-\arctan\left(\frac{H}{S_0}\right), -\arcsin\left(\frac{cd}{2H}\right)\right\}, 0\right) \\ &\cup\left(-\arcsin\left(\frac{c\left(T_c+d\right)}{2H}\right),\right. \\ &\left.-\arcsin\left(\frac{c\left(T_c-d\right)}{2H}\right)\right) \cup \left(0, F_l\left(\frac{cd}{2S}\right)\right) \\ &\cup\left(F_u\left(\frac{c\left(T_c-d\right)}{2S}\right), F_l\left(\frac{c\left(T_c+d\right)}{2S}\right)\right). \end{aligned} \tag{18}$$

Here $F_l(r) = \max_\theta\{\arg_{\varphi_m}(\sin^2((\theta-\varphi_m)/2)/\cos(\varphi_m)) = r\}$; $F_u(r) = \min_\theta\{\arg_{\varphi_m}(\sin^2((\theta-\varphi_m)/2)/\cos(\varphi_m)) = r\}$. For convenience, this relation is marked as $\varphi_m \in \mathbf{\Phi}$. Multipath signals with specific elevation angles can be mitigated by the algorithm. This fact makes it possible to concentrate on some specific parts of elevation angles to provide a better performance.

Therefore, Figure 4 can demonstrate the scale of elevation.

4. Assessment of Multipath Mitigation Performance in GNSS Antennas

Model of multipath signal in GNSS monitoring station has been discussed in Section 2. Effects of multipath mitigation algorithms have been studied in Section 3. Based on those results, an assessment method can be developed to evaluate multipath mitigation ability of antennas. This assessment method is more precise than the legacy front-to-rear ratio approach.

While the installation height H and the minimum distance of inclined reflective surface S_0 are fixed, multipath mitigation performance of antennas can be evaluated by the maximum PPE at every possible elevation angle of multipath signals. We use $G(\gamma) = G_{\text{RHCP}}(\gamma)$ to denote the gain for direct signals at elevation angle γ and use $G_m(\gamma)$ to denote the gain for multipath signals at elevation angle γ. In practice $\alpha = G_m(\gamma)/G(\gamma)$.

Assuming that $\phi_e = 0$ for simplification and double-delta method is adopted in receivers, the maximum PPE at satellite elevation angle θ is shown in

$$\varepsilon_{\max}(\theta) = \max_{\varphi_m}\left\{\varepsilon_{\text{inclined}}\left(\theta, \varphi_m\right), \varepsilon_{\text{horizontal}}\left(\theta\right)\right\}. \tag{19}$$

Here $\varepsilon_{\text{inclined}}(\theta, \varphi_m)$ is the maximum PPE of multipath signals produced by inclined surfaces and $\varepsilon_{\text{horizontal}}(\theta)$ is the maximum PPE of multipath signals produced by horizontal surfaces. $\varepsilon_{\text{inclined}}(\theta, \varphi_m)$ and $\varepsilon_{\text{horizontal}}(\theta)$ are explained in

$$\varepsilon_{\text{inclined}}(\theta, \varphi_m) = \begin{cases} \dfrac{G_m(\varphi_m)}{G_m(\varphi_m) + G(\theta)} \cdot \dfrac{\sin^2(2\varphi_m - \theta)}{\cos(\varphi_m)} \cdot \dfrac{2S_0}{c} & 0 < \dfrac{\sin^2(2\varphi_m - \theta)}{\cos(\varphi_m)} \le \rho_A \\ \dfrac{G_m(\varphi_m)}{G(\theta) - G_m(\varphi_m)} \cdot \left(d - \dfrac{\sin^2(2\varphi_m - \theta)}{\cos(\varphi_m)} \cdot \dfrac{2S_0}{c} \right) & \rho_A < \dfrac{\sin^2(2\varphi_m - \theta)}{\cos(\varphi_m)} \le \dfrac{cd}{2S_0} \\ \dfrac{G_m(\varphi_m)}{2G(\theta) + G_m(\varphi_m)} \cdot \left(d - T_c + \dfrac{\sin^2(2\varphi_m - \theta)}{\cos(\varphi_m)} \cdot \dfrac{2S_0}{c} \right) & \dfrac{c(T_c - d)}{2S_0} < \dfrac{\sin^2(2\varphi_m - \theta)}{\cos(\varphi_m)} \le \rho_B \\ \dfrac{G_m(\varphi_m)}{2G(\theta) - G_m(\varphi_m)} \cdot \left(T_c - \dfrac{\sin^2(2\varphi_m - \theta)}{\cos(\varphi_m)} \cdot \dfrac{2S_0}{c} \right) & \rho_B < \dfrac{\sin^2(2\varphi_m - \theta)}{\cos(\varphi_m)} \le \rho_C \\ \dfrac{G_m(\varphi_m)}{2G(\theta) + G_m(\varphi_m)} \cdot \left(-d - T_c + \dfrac{\sin^2(2\varphi_m - \theta)}{\cos(\varphi_m)} \cdot \dfrac{2S_0}{c} \right) & \rho_C < \dfrac{\sin^2(2\varphi_m - \theta)}{\cos(\varphi_m)} \le \dfrac{c(T_c + d)}{2S_0} \\ 0 & \text{otherwise,} \end{cases} \tag{20}$$

$$\varepsilon_{\text{horizontal}}(\theta) = \begin{cases} \dfrac{G_m(-\theta)}{G(\theta) + G_m(-\theta)} \cdot \dfrac{2H \cdot \sin\theta}{c} & 0 < \dfrac{2H \cdot \sin\theta}{c} \le \tau_A \\ \dfrac{G_m(-\theta)}{G(\theta) - G_m(-\theta)} \cdot \left(d - \dfrac{2H \cdot \sin\theta}{c} \right) & \tau_A < \dfrac{2H \cdot \sin\theta}{c} \le d \\ \dfrac{G_m(-\theta)}{2G(\theta) + G_m(-\theta)} \cdot \left(d - T_c + \dfrac{2H \cdot \sin\theta}{c} \right) & T_c - d < \dfrac{2H \cdot \sin\theta}{c} \le \tau_B \\ \dfrac{G_m(-\theta)}{2G(\theta) - G_m(-\theta)} \cdot \left(T_c - \dfrac{2H \cdot \sin\theta}{c} \right) & \tau_B < \dfrac{2H \cdot \sin\theta}{c} \le \tau_C \\ \dfrac{G_m(-\theta)}{2G(\theta) + G_m(-\theta)} \cdot \left(-d - T_c + \dfrac{2H \cdot \sin\theta}{c} \right) & \tau_C < \dfrac{2H \cdot \sin\theta}{c} \le T_c + d \\ 0 & \text{otherwise.} \end{cases} \tag{21}$$

In this case

$$\begin{aligned} \rho_A &= \frac{cd}{4S_0} \cdot \frac{G(\theta) + G_m(\varphi_m)}{G(\theta)}, \\ \rho_B &= \left[\frac{dG_m(\varphi_m)}{4G(\theta)} + T_c - \frac{d}{2} \right] \cdot \frac{c}{2S_0}, \\ \rho_c &= \left[-\frac{dG_m(\varphi_m)}{4G(\theta)} + T_c + \frac{d}{2} \right] \cdot \frac{c}{2S_0}, \\ \tau_A &= \frac{d}{2} \cdot \frac{G_m(-\theta) + G(\theta)}{G(\theta)}, \\ \tau_B &= \frac{d}{4} \cdot \frac{G_m(-\theta)}{G(\theta)} + T_c - \frac{d}{2}, \\ \tau_c &= -\frac{d}{4} \cdot \frac{G_m(-\theta)}{G(\theta)} + T_c + \frac{d}{2}, \end{aligned}$$

$$\begin{aligned} &\varphi_m \in \mathbf{\Phi}, \\ &\theta \in \left[\theta_{\min}, \frac{\pi}{2} \right]. \end{aligned} \tag{22}$$

$\theta_{\min}$ denotes the minimum satellite elevation angle which is adopted by receivers. Assuming $\arctan(NH/S_0) < \theta_{\min}$, maximum PPE of antenna can be calculated.

Analytical calculations of $\varepsilon_{\max}$ could be tough. In practice, a diagram of ε can simplify the calculation. By plotting $\varepsilon_{\max}(\theta, H, S_0)$ with fixed H and S_0, distribution of the PPE can be demonstrated.

Radiation patterns of practical antennas are measured and displayed in Figure 5 to demonstrate how the proposed assessment method works. In this paper a choke ring antenna designed by Ashtech (mentioned as antenna Ashtech in test) and a Trimble ZEPHYR-Model 2 antenna (mentioned as antenna Trimble in test) are selected in the test. Photos of these two antennas are shown in Figure 6. The maximum

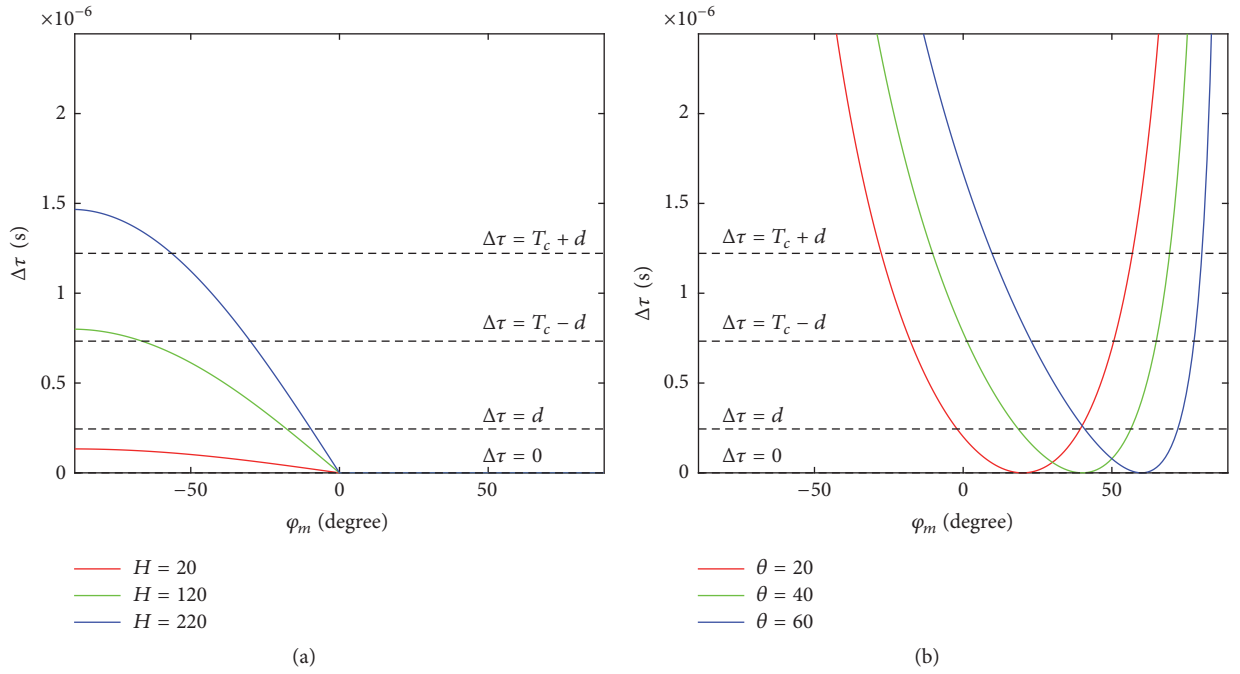

Figure 4: In this figure, the chip width T_c is set to 1/1.023*e*6 as the chip width of C/A code in GPS, the early-late spacing of correlators is $d = 0.25T_c$ and the radius S_0 of semiopen land is 1000 m. (a) shows propagation time delays of multipath signals at horizontal surfaces with different antenna installation heights (H). (b) shows delays at inclined surfaces with different satellite elevation angles (θ). Four horizontal dotted lines marked from top to bottom represent delay thresholds $\Delta\tau = T_c + d$, $\Delta\tau = T_c - d$, $\Delta\tau = d$, and $\Delta\tau = 0$. Only multipath signals with delays between the top two lines and the bottom two lines have impact on PPE.

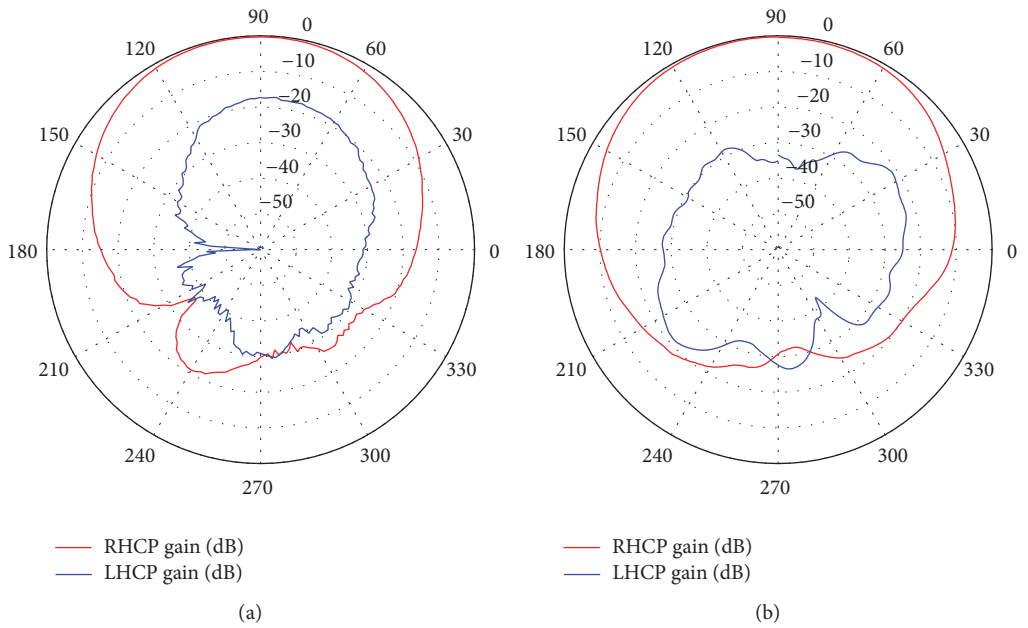

Figure 5: In this figure, all of the data is measured in an anechoic chamber. Elevation angles ranged $(\pi, 2\pi)$ in the figure denote negative elevation angle. (a) is the radiation pattern of antenna Ashtech. (b) is the radiation pattern of antenna Trimble.

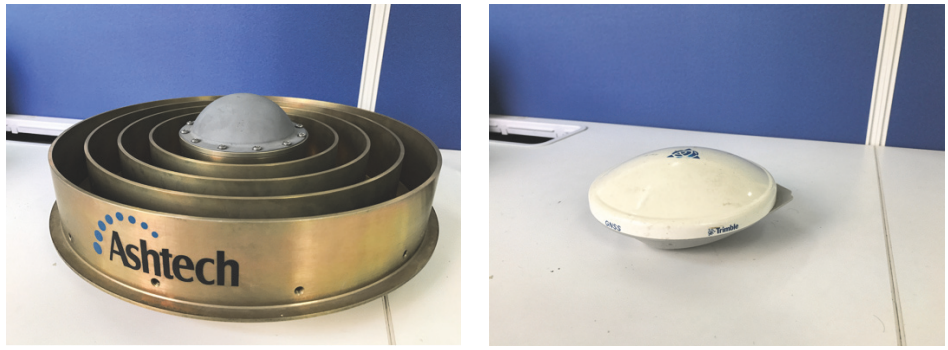

(a) (b)

Figure 6: This photo is the two antennas used in the test. The left one is a chocking ring antenna designed and manufactured by Ashtech. The right one is a Trimble ZEPHYR™-Model 2 antenna.

PPE diagram $\varepsilon(\theta)$ can be plotted based on data collected in an anechoic chamber.

It was mentioned in [19] that the reflection of an electromagnetic wave may change polarization model of the signal. Shift of electric field can be represented via Fresnel reflection coefficient by

$$\rho_{\perp}(\theta_i) = \frac{\cos\theta_i - \sqrt{\varepsilon_2/\varepsilon_1 - \sin^2\theta_i}}{\cos\theta_i + \sqrt{\varepsilon_2/\varepsilon_1 - \sin^2\theta_i}},$$
$$\rho_{\parallel}(\theta_i) = \frac{-(\varepsilon_2/\varepsilon_1)\cos\theta_i + \sqrt{\varepsilon_2/\varepsilon_1 - \sin^2\theta_i}}{(\varepsilon_2/\varepsilon_1)\cos\theta_i + \sqrt{\varepsilon_2/\varepsilon_1 - \sin^2\theta_i}}. \quad (23)$$

Here $\rho_{\perp}$ is the perpendicular reflection coefficient, $\rho_{\parallel}$ is the parallel reflection coefficient, $\varepsilon_2/\varepsilon_1$ is the relative permittivity of the media at the reflection surface, and θ_i is the incidence angle of the direct signal to the surface. In this paper, $\rho_{\perp}$ and $\rho_{\parallel}$ denote reflection coefficient of perpendicular component and parallel component of the direct signal. Most GNSS signals are RHCP signals which have both perpendicular components and parallel components. This difference in reflection coefficients can change the polarization pattern of the multipath signal.

Multipath signals are mainly caused by a reflection form air to soiled materials. Shift in polarization model can be calculated by (23). Polarization model of multipath signal is composed of RHCP component and LHCP component. Hence, total gain of multipath signal is denoted by $G_m(\varphi_m)$ and can be calculated by

$$G_m(\varphi_m) = \alpha_{1,\theta}(\varphi_m)\cdot G_{\mathrm{RHCP}}(\varphi_m) + \alpha_{2,\theta}(\varphi_m)\cdot G_{\mathrm{LHCP}}(\varphi_m). \quad (24)$$

Here $\alpha_{1,\theta}$ and $\alpha_{2,\theta}$ are power distribution of RHCP component and LHCP component. These two parameters can be calculated by (26) and (27). The incidence angle θ_i is calculated via geometry in Section 2 as

$$\theta_i = \frac{\theta - \varphi_m}{2}, \quad (25)$$

$$\alpha_{1,\theta}(\varphi_m) = \left|\frac{\rho_{\parallel}((\theta-\varphi_m)/2) - \rho_{\perp}((\theta-\varphi_m)/2)}{2}\right|, \quad (26)$$

$$\alpha_{2,\theta}(\varphi_m) = \left|\frac{\rho_{\parallel}((\theta-\varphi_m)/2) + \rho_{\perp}((\theta-\varphi_m)/2)}{2}\right|. \quad (27)$$

Given radiation patterns of both antennas, the maximum PPE and the front-to-rear ratio can be plotted. Figure 7 demonstrates the maximum PPE of both antennas at elevation angles range $(0, \pi)$ and provides a comparison with the legacy front-to-rear ratio approach.

We use tolerance of the PPE to evaluate multipath mitigation performance of antennas. The tolerance denotes the maximum PRN code phase error that is acceptable. For a fixed tolerance, there is a range of elevation angle. Within this range, PPE at any elevation angles are below the tolerance. This evaluation represents that there would never be a multipath error which is larger than the tolerance within the range. For a fixed tolerance, a better antenna provides a wider elevation angle range. For a fixed elevation angle range a better antenna provides a lower tolerance instead. The tolerance-based indicator is much more intuitive than the legacy front-to-rear ratio approach.

When the tolerance of the maximum PPE $\bar{\varepsilon}$ is set to $0.05T_c$, both antenna Ashtech and antenna Trimble achieve the requirement at elevation angle range $[4^\circ, 150^\circ]$. When tolerance of PPE $\bar{\varepsilon}$ is set to $0.01T_c$, only antenna Ashtech achieves the requirement at elevation angle range $[30^\circ, 120^\circ]$. This can be a reference to antenna selection. When PPE is not restricted hard, a smaller and cheaper antenna is adoptable with the same performance in multipath mitigation. When high multipath mitigation performance is required, chocking ring antenna is a better choice. Meanwhile the front-to-rear ratio method performs poorly in precise details. From the diagram, it is hard to determine which antenna is better.

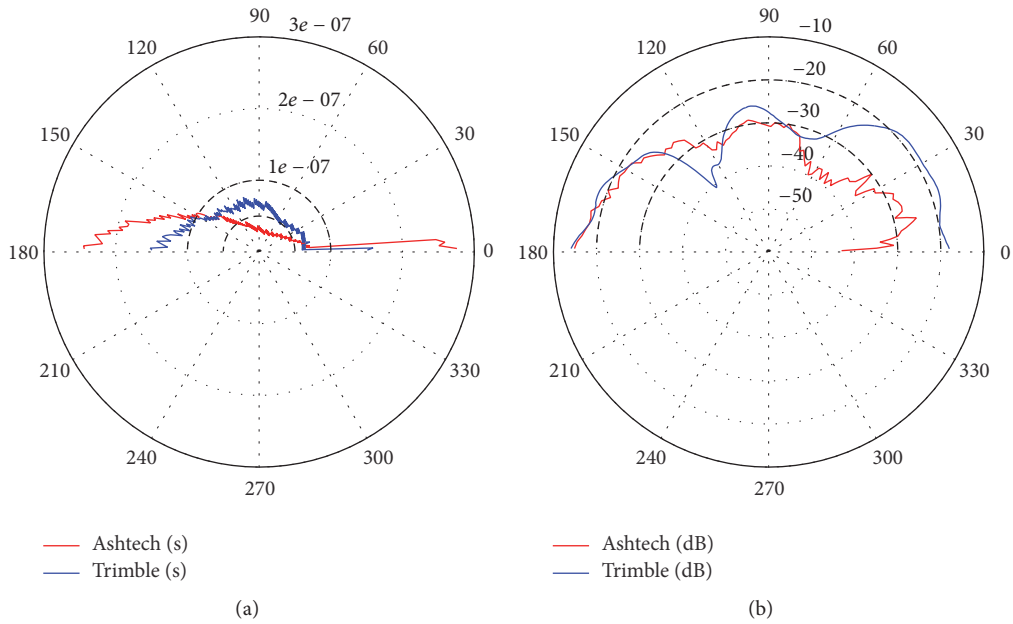

FIGURE 7: In this figure the relative permittivity $\varepsilon_2/\varepsilon_1$ is set experimentally for dry soil surface [19] at $\varepsilon_2/\varepsilon_1 = 3$. Error tolerance of PPE is set to $0.05T_c$ and $0.1T_c$. (a) is the result of proposed assessment method. (b) is the front-to-rear ratio approach. Black dotted circles in (a) are tolerance thresholds.

With conclusion in this section, antennas can be designed to match multipath mitigation algorithm. A matched design may be a reinforcement of the multipath mitigation performance of the receiver.

5. Site Dependence for Monitoring Antennas

The model of multipath signals at GNSS monitoring station has been analyzed in Section 2. Site selection of the antenna can be optimized via methods proposed above. Given the radiation pattern of a monitoring antenna and the multipath mitigation algorithm in the receiver, it is possible to mitigate multipath effects by adjusting the installation site of the antenna. In this section, the height of the antenna and the radius of the open area will be discussed separately.

5.1. Installation Height of Antennas. Heights of antennas mainly influence mitigation performance in multipath signals produced by horizontal reflective surfaces. The PPE in this scenario can be calculated via conclusions in Section 2. We use $\mathrm{PH}_{\max}$ to denote the maximum PPE when parameter H is alterable and use $\mathrm{PH}_{\mathrm{avg}}$ to denote the average PPE when parameter H is alterable.

$$\mathrm{PH}_{\max}(H) = \max_{\theta} |\varepsilon(\theta, H)|, \quad \theta \in \left[\theta_{\min}, \frac{\pi}{2}\right],$$
$$\mathrm{PH}_{\mathrm{avg}}(H) = \frac{1}{\pi/2 - \theta_{\min}} \int_{\theta_{\min}}^{\pi/2} |\varepsilon(\theta, H)|\, d\theta. \tag{28}$$

Here $\varepsilon(\theta, H)$ is represented in (21) in Section 4. Results of practical antennas mentioned in Section 4 can demonstrate the method. Characteristics of the PPE along with the change of H can be plotted as Figure 8.

There are some discontinuities in Figure 8. This phenomenon is the result of those discontinuities in (21) and the effective angle range shown in (18). When the height of antenna reaches some thresholds, propagation delay of multipath signal may fall into the space between the second and the third dotted line in Figure 4. Some of these delays have no impact on multipath error because there are not any multipath signals at these delays. When the height of the antenna increases, the elevation angle of the multipath signal with the maximum PPE may change.

Form Figure 8 both the maximum and the average PPE increase with H first and then decrease. It can be found that the best height selection of antenna installation is zero. This conclusion is right under the situation that only horizontal reflective surfaces are considered. In practice, a higher installation height can provide a larger radius of semiopen land, which can effectively reduce the multipath error caused by inclined surfaces. From Figure 9 we can figure out that the PPE of multipath signals at inclined surfaces are larger than the PPE at horizontal surfaces. In the process of site selection, there is a tradeoff between the height and the radius.

An impropriate height may cause a larger error. For a fixed tolerance of maximum or average PPE, the proper range of height can be determined by this method. Detailed phase error diagram with elevation angles can be a reference for the selection of the height H.

From Figure 9, errors caused by multipath signals can be eliminated well in large elevation angles when height H is large (the blue line). However, an antenna with a limited installation height is much easier to deploy. Thus, it can

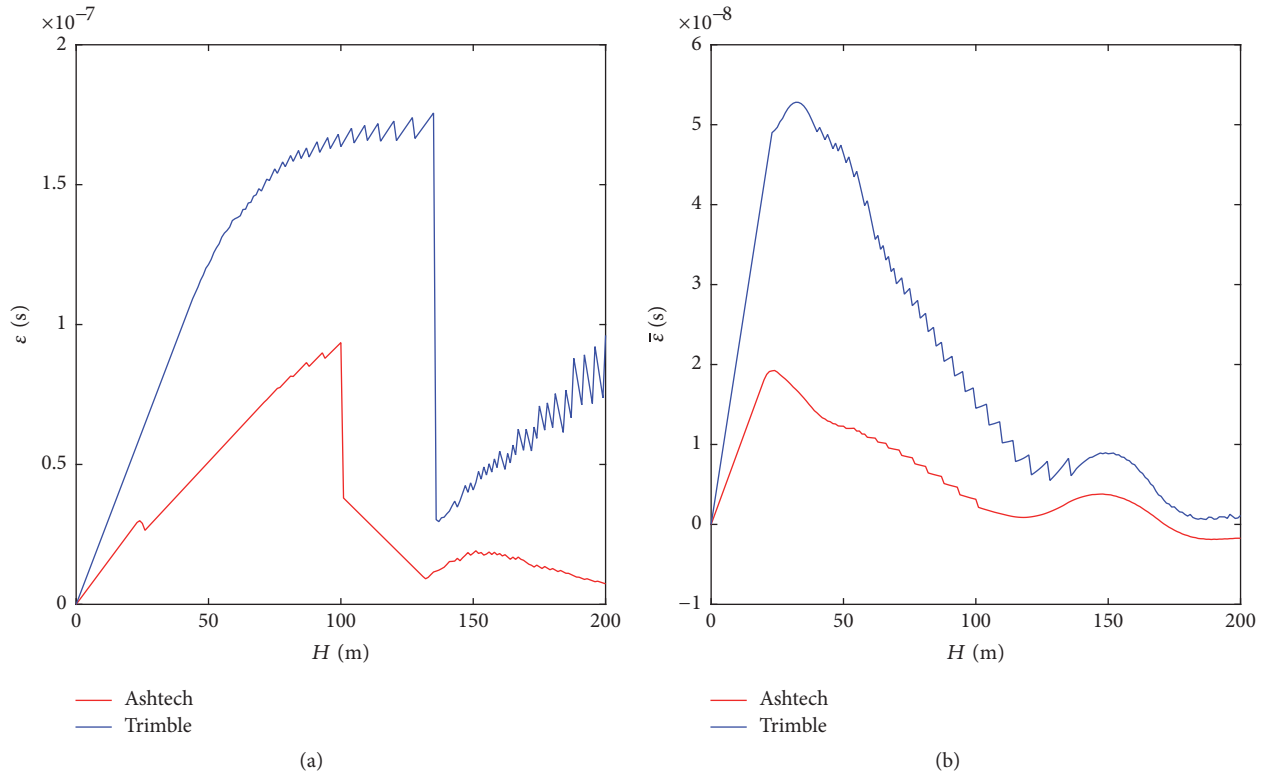

FIGURE 8: This figure shows how the PPE varies with the antenna height H. In this figure, the width T_c of the chip is set to 1/1.023*e*6 as the chip width of C/A code in GPS; the interval of correlators is $d = 0.25T_c$. (a) is the maximum PPE. (b) is the average PPE.

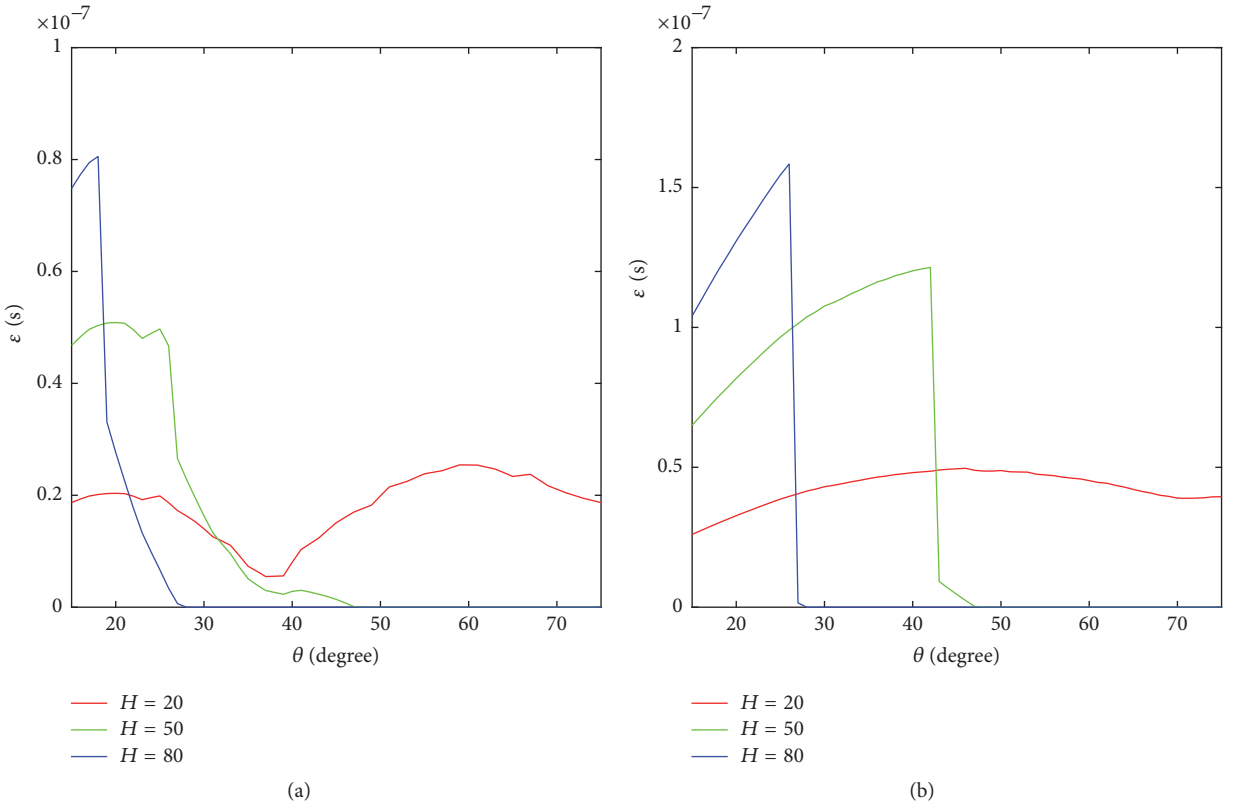

FIGURE 9: This figure shows the variety of the PPE with the satellite elevation angle θ. In this figure, the width T_c of chip is set to 1/1.023*e*6 as the C/A code in GPS; the interval of correlators is $d = 0.25T_c$. (a) is the result of antenna Ashtech. (b) is result of antenna Trimble.

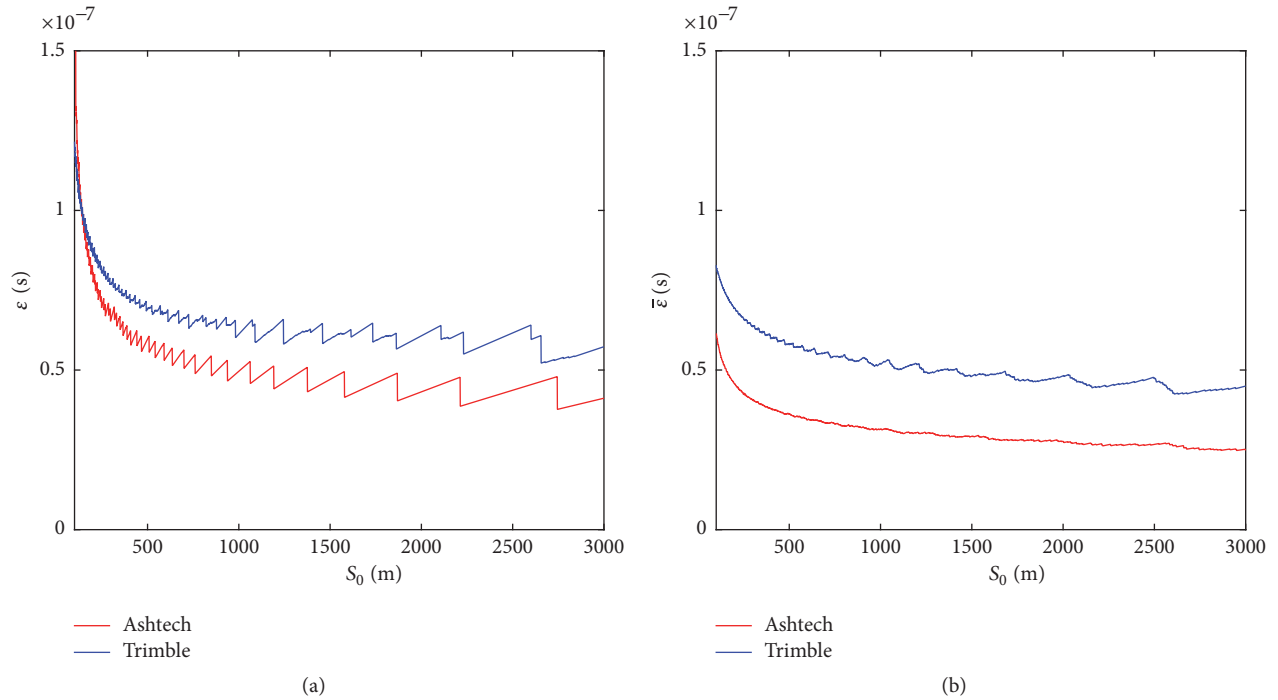

FIGURE 10: This figure shows the variety of PS_{max} and PS_{avg} with S_0. In this figure, the width T_c of chip is set to 1/1.023*e*6 as the chip width of C/A code in GPS, the interval of correlators is $d = 0.25T_c$. (a) is the result of antenna Ashtech. (b) is the result of antenna Trimble.

reduce the difficulty of installation (the red line) and maintain an acceptable error level.

5.2. Radius of Open Area. The radius of the open area has effects on mitigating multipath signals caused by inclined reflective surfaces. The PPE in this scenario can be calculated via conclusion in Section 4. We use PS_{max} to denote the maximum PPE when parameter S_0 is alterable and use PS_{avg} to denote average PPE when parameter S_0 is alterable.

$$\begin{aligned} \mathrm{PS}_{\max}(S_0) &= \max_{\theta,\varphi_m} \left|\varepsilon(\theta,\varphi_m,S_0)\right|, \\ &\qquad \theta \in \left[\theta_{\min}, \frac{\pi}{2}\right], \ \varphi_m \in \mathbf{\Phi}, \\ \mathrm{PS}_{\mathrm{avg}}(S_0) &= \frac{1}{\pi} \cdot \frac{1}{\pi/2 - \theta_{\min}} \int_{\theta_{\min}}^{\pi/2} \int_{-\pi/2}^{\pi/2} \left|\varepsilon(\theta,\varphi_m,S_0)\right| d\varphi_m \, d\theta, \\ &\qquad \theta \in \left[\theta_{\min}, \frac{\pi}{2}\right], \ \varphi_m \in \mathbf{\Phi}. \end{aligned} \tag{29}$$

Here $|\varepsilon(\theta, \varphi_m, S_0)|$ is represented in (20) in Section 4. Results of practical antennas mentioned in Section 4 can demonstrate the method. When the early-late spacing d and chip width T_c are fixed in double-delta algorithm, the maximum and the average PPE can be plotted as Figure 10.

From Figure 10 both the maximum and the average error decrease by the increase of the radius S_0. There is also an oscillation in the short range with the variety of S_0. For a fixed tolerance of the maximum or the average PPE, the minimum radius of open area can be determined by the conclusion above.

6. Assessment under Other Algorithms and Modulations

We pick double-delta algorithm under BPSK modulation as an example to analyze multipath mitigation in this paper. There are many other algorithms and modulations in GNSS application. In this section, we make a brief of how the proposed assessment method works in other algorithms and modulations.

6.1. Assessment under Other Multipath Mitigation Algorithms. Besides the double-delta approach, there are many other algorithms for multipath mitigation. The narrow correlator and the early-late slope are also multipath mitigation algorithms applied in receivers. These algorithms are mainly different with the double-delta approach in the expression of PRN code phase error function. For example, (30) is the PRN code phase error function of narrow correlator.

$$\varepsilon(\alpha, \Delta\tau, \Delta\phi) = \begin{cases} \dfrac{\alpha \cdot \cos\Delta\phi}{1 + \alpha \cdot \cos\Delta\phi} \cdot \Delta\tau & 0 < \Delta\tau \le \tau_L \\ \dfrac{\alpha d}{2} \cdot \cos\Delta\phi & \tau_L < \Delta\tau \le \tau_H \\ \dfrac{\alpha \cdot \cos\Delta\phi}{2 - \alpha \cdot \cos\Delta\phi} \cdot \left(T_c + \dfrac{d}{2} - \Delta\tau\right) & \tau_H < \Delta\tau \le T_c + \dfrac{d}{2} \\ 0 & T_c + \dfrac{d}{2} < \Delta\tau, \end{cases} \tag{30}$$

where τ_L is defined in (31) and τ_H is defined in (32).

$$\tau_L = \frac{1 + \alpha \cdot \cos \Delta\phi}{2} \cdot d, \tag{31}$$

$$\tau_H = \frac{\alpha d}{2} \cdot \cos \Delta\phi + T_c - \frac{d}{2}. \tag{32}$$

The proposed assessment method can shift to the narrow correlator algorithm by replacing (14) with (30) in calculation of PRN code phase error. Different algorithms may lead to different assessment results but the method still works.

Hence, the proposed method can also be adopted to help select a proper multipath mitigation algorithm for a certain type of antenna. We can run the proposed assessment for the same antenna under different multipath mitigation algorithms to find the best algorithm to match the radiation pattern of the antenna.

6.2. Assessment under Other Modulations. The BOC is adopted in modern GPS signals. Different from BPSK, the primary correlation peak of the BOC signal is more narrow than BPSK. Hence, early-late spacing d has a stricter range for value selection.

Double-delta approach is based on the evaluation of slopes on both sides of the primary correlation peak of the receiving signal. The space between E2 and L2 ($2d$) should be lower than the width of the primary correlation peak. When modulation method is BOC(m, n), (33) shows the constraint condition of the early-late spacing d.

$$d \leq \frac{T_c}{k}. \tag{33}$$

Here $k = 2m/n$ is the number of bit flopping of BOC in a single chip of the PRN code. If this spacing is supported in the algorithm, our method is still available.

Hence, the proposed method is still available when the multipath mitigation algorithm is available under other modulations.

7. Conclusion

In this paper, we studied the model of multipath signals in GNSS monitoring stations. The involving of inclined reflective surfaces increases the precision of the multipath model in semiopen areas. The calculation of multipath delay shows that multipath signals will only happen at a specific range of elevation angles. This range can be expressed by a function of signal properties and environment characteristics.

Multipath mitigation algorithms were studied. By deploying multipath mitigation algorithm, certain ranges of multipath signals can be eliminated. This range can be calculated via arguments of the modulation and the algorithm. Thus, specific elevation angles of antennas may be ignored to enhance performance for antenna design.

We calculated the results of two practical antennas. An accurate approach to evaluate the multipath mitigation performance for antennas is proposed. With the method, developers may assess antennas in a precise way.

We simulated different installation sites of antennas. Principles for site selection are introduced based on methods proposed above. Effects of antenna height and semiopen land radius are analyzed. A proper range of both arguments is put forward to optimize the site. With these principles effects caused by multipath can be mitigated.

We also analyze the availability of the proposed method under other algorithms and modulations. The result shows that our method still works under most major algorithms and modulations in GPS applications.

Abbreviations

GNSS: Global Navigation Satellite System
DLL: Delay lock loop
PPE: The PRN code phase error
GPS: Global positioning system
MEDLL: Multipath estimating delay lock loop
MMT: Maximal measurement tree
RHCP: Right-hand circular polarization
LHCP: Left-hand circular polarization.

Conflicts of Interest

The authors declare that there are no conflicts of interest regarding the publication of this paper.

References

[1] E. D. Kaplan and C. J. Hegarty, "Interference, multipath, and scintillation," in *Understanding GPS: Principles and Applications*, pp. 279–294, Artech House, Boston, Mass, USA, 2nd edition, 2006.

[2] R. D. J. Van Nee, "Spread-spectrum code and carrier synchronization errors caused by multipath and interference," *IEEE Transactions on Aerospace and Electronic Systems*, vol. 29, no. 4, pp. 1359–1365, 1993.

[3] M. Irsigler, "Characterization of multipath phase rates in different multipath environments," *GPS Solutions*, vol. 14, no. 4, pp. 305–317, 2010.

[4] V. U. Zavorotny, K. M. Larson, J. J. Braun, E. E. Small, E. D. Gutmann, and A. L. Bilich, "A physical model for GPS multipath caused by land reflections: toward bare soil moisture retrievals," *IEEE Journal of Selected Topics in Applied Earth Observations and Remote Sensing*, vol. 3, no. 1, pp. 100–110, 2010.

[5] C. C. Chew, E. E. Small, K. M. Larson, and V. U. Zavorotny, "Effects of near-surface soil moisture on GPS SNR data: development of a retrieval algorithm for soil moisture," *IEEE Transactions on Geoscience and Remote Sensing*, vol. 52, no. 1, pp. 537–543, 2014.

[6] K. Fan and X. Ding, "Estimation of GPS carrier phase multipath signals based on site environment," *Journal of Global Positioning Systems*, vol. 5, no. 1, pp. 22–28, 2006.

[7] A. J. Van Dierendonck, P. Fenton, and T. Ford, "Theory and performance of narrow correlator spacing in a GPS receiver," *Navigation, Journal of the Institute of Navigation*, vol. 39, no. 3, pp. 265–283, 1992.

[8] B. Townsend and P. Fenton, "A practical approach to the reduction of pseudorange multipath errors in a L1 GPS receiver," in *Proceedings of the 7th International Technical Meeting of the*

Satellite Division of the Institute of Navigation (ION GPS '94), pp. 143–148, Salt Lake City, Utah, USA, September 1994.

[9] L. Garin, J. L. Rousseau et al., "Strobe and edge correlator multipath mitigation for code," in *Proceedings of the 9th International Technical Meeting of the Satellite Division of The Institute of Navigation (ION GPS '96)*, pp. 657–664, Kansas City, Mo, USA, September 1996.

[10] G. A. Mcgraw and M. S. Braasch, "GNSS multipath mitigation using gated and high resolution correlator concepts," in *Proceedings of the 1999 National Technical Meeting of The Institute of Navigation*, pp. 333–342, San Diego, Calif, USA, January 1999.

[11] J. Jones, P. Fenton, B. Smith et al., Theory and Performance of the Pulse Aperture Correlator, Pulse Aperture Correlator 2004.

[12] R. Hatch, R. Keegan, T. A. Stansell et al., "Leica's code and phase multipath mitigation techniques," in *Proceedings of the 1997 National Technical Meeting of The Institute of Navigation*, pp. 217–225, Santa Monica, Calif, USA, January 1997.

[13] M. Irsigler and B. Eissfeller, "Comparison of multipath mitigation techniques with consideration of future signal structures," in *Proceedings of the 16th International technical Meeting of the Satellite Division of the Institute of Navigation (ION GPS/GNSS '03)*, pp. 2584–2592, Portland, Ore, USA, September 2003.

[14] R. D. J. van Nee, J. Siereveld, P. C. Fenton, and B. R. Townsend, "Multipath estimating delay lock loop: approaching theoretical accuracy limits," in *Proceedings of the IEEE Position Location and Navigation Symposium*, pp. 246–251, Las Vegas, Nev, USA, April 1994.

[15] P. C. Fenton and J. Jones, "The theory and performance of NovAtel Inc.'s Vision Correlator," in *Proceedings of the 18th International Technical Meeting of the Satellite Division of The Institute of Navigation (ION GNSS '05)*, pp. 2178–2186, Long Beach, Claif, USA, September 2005.

[16] P. Closas, C. Fernández-Prades, and J. A. Fernández-Rubio, "A Bayesian approach to multipath mitigation in GNSS receivers," *IEEE Journal on Selected Topics in Signal Processing*, vol. 3, no. 4, pp. 695–706, 2009.

[17] M. Sahmoudi and M. G. Amin, "Fast Iterative Maximum-Likelihood Algorithm (FIMLA) for multipath mitigation in the next generation of GNSS receivers," *IEEE Transactions on Wireless Communications*, vol. 7, no. 11, pp. 4362–4374, 2008.

[18] B. R. Rao, W. Kunysz, R. Fante, and K. McDonald, "Antennas and Site Considerations for Precise Applications," in *GPS/GNSS Antennas*, pp. 362–370, Artech House, Boston, Mass, USA, 2013.

[19] L. Lau and P. Cross, "Development and testing of a new ray-tracing approach to GNSS carrier-phase multipath modelling," *Journal of Geodesy*, vol. 81, no. 11, pp. 713–732, 2007.

[20] H. Liu, X. Li, L. Ge, C. Rizos, and F. Wang, "Variable length LMS adaptive filter for pseudorange multipath mitigation based on SydNET stations," *Journal of Applied Geodesy*, vol. 3, no. 1, pp. 35–46, 2009.